Inorganic Chemistry

Article

pubs.acs.org/IC

Unique Optical Oxygen-Sensing Performance of $[Ru(IP)_2(HNAIP)]^{2+}$ during the Groove-Binding-Induced B-to-Z DNA Conformational Transition

Linlin Chen,[†] Hui Chao,[‡] Qianwen Zhao,[†] and Hong Li*[,†]

[†]School of Chemistry and Environment, South China Normal University, Guangzhou 510006, P. R. China

[‡]Department of Chemistry, Sun Yat-Sen University, Guangzhou 510275, P. R. China

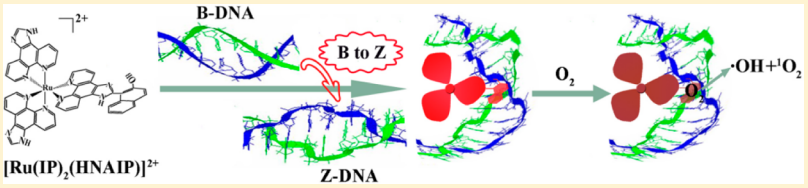

ABSTRACT: The oxygen-sensing performance of $[Ru(IP)_2(HNAIP)]^{2+}$ (Ru1, IP = imidazo[4,5-*f*][1,10]phenanthroline and HNAIP = 2-(2-hydroxy-1-naphthyl)imidazo [4,5-*f*][1,10]phenanthroline) in the presence of DNA conformational transition has been investigated by means of absorption spectroscopy, steady-state and time-resolved fluorescence spectroscopies, and circular dichroism spectroscopy. Ru1 shows a good linear response toward oxygen between pure nitrogen and pure oxygen with an on−off emission intensity ratio (I_0/I_{100}) of up to 9.3 via a dynamic quenching mechanism. Compared with $[Ru(IP)_2(DHPIP)]^{2+}$ (Ru2, DHPIP = 2-(2,4-dihydroxyphenyl)imidazo[4,5-*f*][1,10]phenanthroline, I_0/I_{100} = 5.8), the HNAIP ligand endows Ru1 with favorable oxygen binding sites to achieve larger energy and electron transfer rates. Simultaneously, Ru1 can induce the B-to-Z DNA conformational transition via a groove interaction with an intrinsic binding constant (K_b) of 7.9×10^4 M^{-1}, whereas there is no same phenomenon for Ru2 intercalated into DNA ($K_b = 3.3 \times 10^5$ M^{-1}). Furthermore, the B-to-Z DNA conformational transition is interestingly found to decrease the Ru1-based oxygen-sensing rate by about 33%.

1. INTRODUCTION

DNA is a very important macromolecule for all known living organisms and many viruses.[1] Although the right-handed double helical DNA (B-DNA) is most commonly found in cells, another kind of left-handed DNA (Z-DNA), in which the double helix winds to the left in a zigzag pattern, has directly emerged in functional organisms[2,3] and is necessary for many biological processes.[4] However, the Z-DNA with a higher energy level than B-DNA is difficult to stably exist in an aqueous medium.[5] Some metal complexes, synthetic organic compounds, polyamines, proteins, peptides, and oligonucleotides have been used to stabilize the Z-DNA conformation.[6,7] Because polypyridyl ruthenium(II) complexes possess rich photochemical and photophysical properties, they have been used as the promising recognition agents to bind DNA via classic intercalation, partial intercalation, groove binding, and/or electrostatic attraction.[8,9] Recently, Cardin and co-workers have reported an atomic resolution X-ray crystal structure of *rac*-$[Ru(phen)_2(dppz)]^{2+}$ (1,10-phenanthroline and dppz (dipyrido[3,2,-*a*:2′,3′-*c*]phenazine) with $d(ATGCAT)_2$, showing different orientations of the Λ and Δ binding sites.[10] Among the DNA-binding modes, the groove binding of Ru(II) complexes to DNA has been known to possibly induce the DNA conformational transition, resulting in the Z-DNA stabilized by Ru(II) complexes.[11,12] As we know, the DNA always exists in an oxygen-containing environment.[13] Therefore, it is of considerable interest to know the interactions among DNA, Ru(II) complexes, and oxygen.

Some of the polypyridyl Ru(II) complexes have also been regarded as potential photosensitizers for optical oxygen-sensing applications.[14,15] Several researchers have reported the oxygen-sensing behavior of $[Ru(bpy)_3]^{2+}$ (bpy = 2,2′-bipyridine) assembled in a polymer matrix, sol−gel derived silica, or mesoporous silicate as quantitatively described by eq 1[16−19]

$$\frac{I_0}{I} = \frac{\tau_0}{\tau} = 1 + K_{SV}C_{O_2} \quad (1)$$

where I_0 and τ_0 are the initial emission intensity and lifetime of Ru(II) complexes in an inert atmosphere, and I and τ are the emission intensity in the presence of oxygen. K_{SV} is the Stern−Volmer quenching constant, and C_{O_2} represents the oxygen concentration. In addition to $[Ru(bpy)_3]^{2+}$, the oxygen-sensing performances of other Ru(II) complexes bearing π-conjugated aromatic ligands have been extensively studied, showing the quenching of ^{3}MLCT (triplet metal-to-ligand charge transfer) excited states by oxygen.[20,21] $[Ru(dpp)_3]^{2+}$ (dpp = tris(4,7-diphenyl-1,10-phenanthroline)) doped in fluorinated xerogels has shown the highly sensitive oxygen-sensing performance,[22] which was superior to those of $[Ru(bpy)_3]^{2+}$ and [Ru-

Received: April 16, 2015
Published: August 17, 2015

DOI: 10.1021/acs.inorgchem.5b00862
Inorg. Chem. 2015, 54, 8281−8287

$(phen)_3]^{2+}$.[23] So far, there have been many studies on the optical oxygen-sensing characteristics of a series of Ru(II) complexes by the contribution of ^{3}IL (triplet intraligand) excited energy to the ^{3}MLCT emissive states.[24,25] Despite the fact that polypyridyl Ru(II) complexes have been extensively used as luminescent probes of both oxygen sensing and DNA structure,[26,27] there is no report on the oxygen-sensing characteristics of Ru(II) complexes bound to the groove surface of a DNA duplex with the B-to-Z conformational transition.

In our previous studies, a di-Ru(II) complex $[Ru(bpy)_2(mbpibH_2)(bpy)_2Ru]^{4+}$ bearing a flexible V-shaped bridging ligand (mbpib = 1,3-bis([1,10]phenanthroline[5,6-*d*]imidazol-2-yl)benzene) has been demonstrated to induce the condensation of DNA with the B-to-Z conformation transition via a groove-binding mode.[28] Two intramolecular hydrogen-bond-containing mono-Ru(II) complexes $[Ru(bpy)_2(HNAIP)]^{2+}$ and $[Ru(bpy)_2(HPIP)]^{2+}$ (HNAIP = 2-(2-hydroxy-1-naphthyl)-imidazo[4,5-*f*][1,10]phenanthroline and HPIP = (2-(2,4-dihydroxyphenyl)imidazo[4,5-*f*][1,10]phenanthroline) have been known to bind DNA by two binding modes.[29] Compared with the HPIP ligand, the HNAIP ligand has a unique naphthyl ring and a rotatable C−C single bond between 2-hydroxynaphthalene and imidazo[4,5-*f*][1,10]phenanthroline (IP), leading to a very different DNA-binding mode. In addition, if the IP ligand was used to replace the two bpy ancillary ligands, the binding interaction of $[Ru(IP)_2(dppz)]^{2+}$ with DNA was enhanced.[30] In the current work, we concentrate on the interesting oxygen-sensing performances of two novel Ru(II) complexes $[Ru(IP)_2(HNAIP)]^{2+}$ and $[Ru(IP)_2(DHPIP)]^{2+}$ (DHPIP = 2-(2,4-dihydroxyphenyl)imidazo[4,5-*f*][1,10]phenanthroline) bound to DNA. Meanwhile, an important effort is made to demonstrate the effects of the B-to-Z DNA conformational transition on the oxygen-sensing performances of polypyridyl Ru(II) complexes.

2. EXPERIMENTAL SECTION

2.1. Chemicals and Materials. Tris(hydroxylmethyl)-aminomethane (Tris) from Sigma was used to prepare buffer solutions with doubly distilled water, consisting of 0.01 M Tris/0.05 M NaCl (pH 7.2). Herring sperm DNA (Qiyun Co., China) was used as received. HNAIP, DHPIP, IP, and their racemic Ru(II) complexes including $[Ru(IP)_2(HNAIP)]Cl_2$ (Ru1) and $[Ru(IP)_2(DHPIP)]Cl_2$ (Ru2) were synthesized and characterized following previously reported procedures,[29−31] and the structures of Ru1 and Ru2 are shown in Figures 1 and 2, respectively. ***Caution!*** *Perchlorate salts of metal complexes with organic ligands are potentially explosive. Only small amounts of the material should be prepared and handled with great care.* To examine the presence of various forms of oxygen radicals, the concentration of Ru(II) complexes was selected as 10 μM. L-Histidine (His, from nonanimal source), dimethyl sulfoxide (DMSO), and superoxide dismutase (SOD, from bovine erythrocytes) were used as scavengers against singlet oxygen, hydroxyl radical, and superoxide anion, respectively, and the quenching-recovered efficiency (*QRE*) is defined as eq 2

$$QRE = \frac{I' - I'_0}{I_0 - I} \times 100\% \quad (2)$$

where I_0 and I are Ru(II) complex-based emission intensities under nitrogen and oxygen atmospheres. I'_0 and I' are emission intensities under oxygen atmospheres in the absence and presence of scavengers added within 2 min, respectively.

2.2. Experimental Methods and Conditions. Electronic absorption spectra were recorded on a UV-1700 spectrophotometer (Shimadzu, Japan). Steady-state emission survey was performed on a

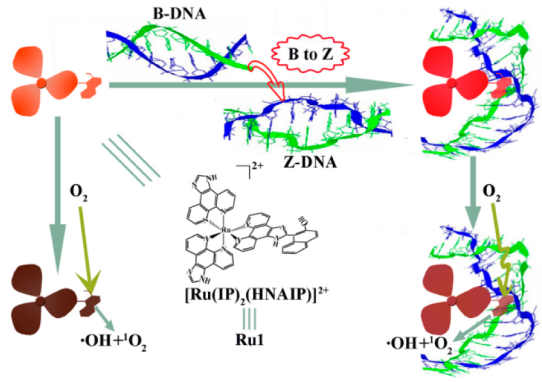

Figure 1. Schematic diagrams for illustrating the effects of Z-DNA conformation on the oxygen emission quenching of Ru1. Inset shows the structure of Ru1.

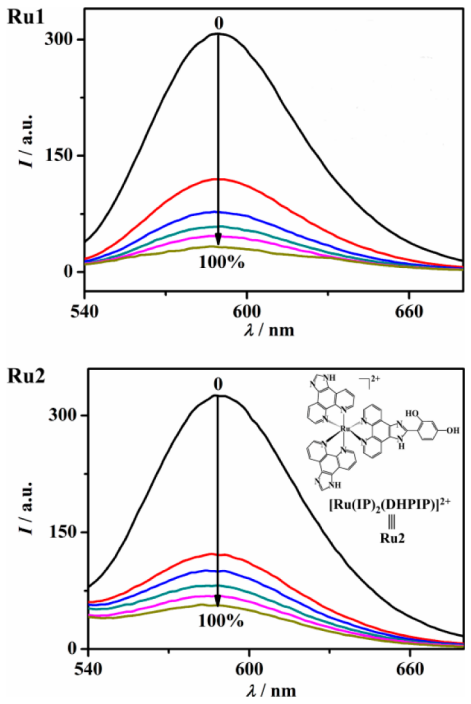

Figure 2. Emission spectra of 10 μM Ru1 or Ru2 upon increasing oxygen concentration (C_{O_2} = 0, 20, 40, 60, 80, and 100%). Inset shows the structure of Ru2.

Hitachi RF-2500 fluorescence spectrophotometer. The excitation wavelength of 450 nm was used. Time-resolved emission measurement was carried out by an Edinburgh Instruments FLS920 combined fluorescence lifetime spectrometer.[32] The lifetimes of Ru(II) complexes in the absence and presence of DNA were defined as τ_{Ru} and $\tau_{Ru\text{-}DNA}$, which were obtained by the single and double exponential fitting for emission decay traces, respectively. $\tau_{Ru\text{-}DNA}$ was calculated by eq 3.

$$\tau_{Ru\text{-}DNA} = A_1 \times \tau_s + A_2 \times \tau_l \quad (3)$$

Herein, τ_s and τ_l are the short and long lifetime components, in which the percentage of the emission are A_1 and A_2, respectively. Circular dichroism (CD) spectra of 0.04 mM DNA in the absence and presence of Ru1 or Ru2 were measured using a JASCO J-810 spectropolarimeter. Machine plus cuvettes baselines of buffer solutions were subtracted. Each spectrum was scanned between 225 and 325 nm and was collected after averaging over three accumulations at 25 °C. The oxygen-sensing measurement was performed in a hermetical quartz cuvette filled with buffer solutions containing different

DOI: 10.1021/acs.inorgchem.5b00862
Inorg. Chem. 2015, 54, 8281−8287

concentrations of oxygen via two gas-flow controllers from pure oxygen and nitrogen. All the experiments were performed at room temperature (19−22 °C) unless otherwise noted.

3. RESULTS AND DISCUSSION

3.1. Oxygen-Sensing Performance of Ru1 and Ru2. An ideal fluorescent probe should possess long-term stability, high sensitivity, and appropriate emission response.[33] Figure 2 shows the emission spectra of Ru1 at various oxygen concentrations upon the excitation of 450 nm light, indicating an intense emission peak at 588 nm from Ru(II)-based ^{3}MLCT excited states under a pure nitrogen atmosphere. When a pure nitrogen atmosphere was replaced by oxygen, the emission intensity ratio (I_0/I_{100}) was determined to be 9.3, which is larger than those of most optical oxygen sensors hitherto reported.[17,34−36] In the oxygen concentration range between pure nitrogen and pure oxygen, the emission shows a continuous decrease, and a linear Stern−Volmer plot is achieved with a regression coefficient (R) of 0.996, as depicted by Figure 3. The quenching constant (K_{SV}) is 0.080 %$^{-1}$, taken as an average of three parallel experiments with a relative standard deviation (RSD) of 2.8% (n = 3). Compared with the multisite emission quenching,[37,38] the Ru1 luminophores show a good linear response toward oxygen with high sensitivity and reproducibility.

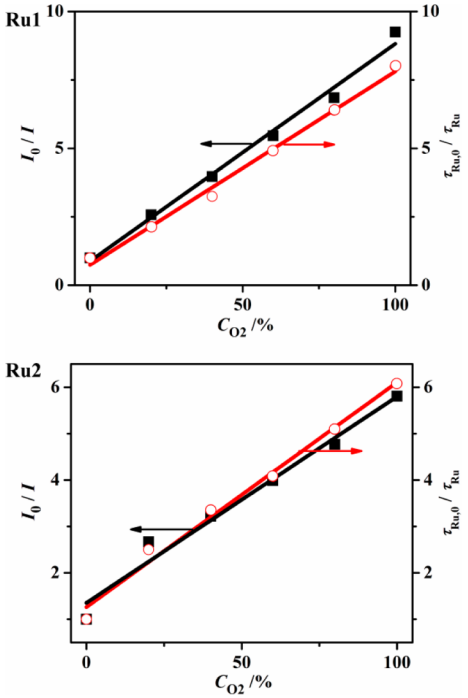

Figure 3. Emission intensity ratio (I_0/I, left) and lifetime ratio ($\tau_{Ru,0}/\tau_{Ru}$, right) of 10 μM Ru1 or Ru2 under pure nitrogen and oxygen atmosphere as a function of C_{O_2}.

To further illustrate the contribution of the HNAIP ligand to the Ru1-based oxygen sensing, Ru1 was changed to Ru2 to perform the measurement of emission spectra under analogous conditions. As depicted by Figures 2 and 3, the I_0/I_{100} ratio and K_{SV} are 5.8 and 0.044 %$^{-1}$, respectively, which are smaller than those of Ru1, suggesting that the HNAIP ligand possessing a 2-hydroxynaphthalene unit endows Ru1 with a high oxygen-sensing sensitivity. To know the quenching mechanism by oxygen, the time-resolved emission spectra of Ru1 and Ru2 were measured upon increasing oxygen contents. While fitting the emission decay traces with a single exponential mode, the resultant lifetimes are shown in Figure 3. The excited-state lifetime ratio ($\tau_{Ru,0}/\tau_{Ru}$) under pure nitrogen- and oxygen-containing atmospheres is basically equal to the corresponding I_0/I, both of which show a good linear increase within increasing oxygen concentration, suggesting a dynamic quenching mechanism.[39] The k_q values are 8.4 × 10^4 %$^{-1}$ s^{-1} and 4.4 × 10^4 %$^{-1}$ s^{-1} for Ru1 and Ru2, respectively, revealing that Ru1 has a larger oxygen quenching rate.

While using His, SOD, and DMSO to examine the presence of singlet oxygen, superoxide anion, and hydroxyl radicals, respectively,[40,41] as depicted in Table 1, Ru1 and Ru2 can photoinduce molecular oxygen to produce singlet oxygen and hydroxyl radicals. The results demonstrate that there exists the energy and electron transfer between photoexcited Ru(II) complexes and ground-state oxygen. In addition, the emission spectra of Ru1 and Ru2 under a nitrogen atmosphere show a consistent emission peak at 588 nm, suggesting that the two complexes possess an approximate lowest unoccupied molecular orbital (LUMO) energy level centered on the HNAIP and DHPIP ligands.[42] However, a comparison of the two ligands suggests that 2-hydroxynaphthalene end-capped the IP ligand (HNAIP) existing in the photoexcited Ru1 provides a more favorable binding site for oxygen molecules compared with the resorcinol unit in the DHPIP,[43] making the I_0/I_{100} ratio of Ru1 increase to 9.3.

3.2. DNA-Binding Behavior of Ru1 and Ru2. In addition to the oxygen sensing, the binding properties of Ru1 and Ru2 to DNA are comparatively investigated. Figure 4 shows three intraligand (IL) bands at 230−400 nm and a broad MLCT absorption band in the visible region of 400−500 nm.[44] The MLCT absorption peak shows a pronounced hypochromism and red shift upon increasing DNA concentration. According to eqs 4a and 4b,[45] the DNA binding constant K_b and binding site size in base pairs (s) are further calculated

$$(\varepsilon_a - \varepsilon_f)/(\varepsilon_b - \varepsilon_f) = (b - (b^2 - 2K_b^2 C_{Ru} C_{DNA}/s)^{1/2})/2K_b C_{Ru} \quad (4a)$$

Table 1. Protective Effects of His, DMSO, and SOD Added within 2 min against Singlet Oxygen, Hydroxyl Radical, and Superoxide Anion Derived from Molecular Oxygen upon Incorporation of 10 μM Ru1 or Ru2. *QRE*, λ_{Em}, and K_{SV} Represent the Quenching-Recovered Efficiencies, Max Emission Wavelength, and Stern−Volmer Quenching Constant

	QRE/%				
systems	+ His (1 mM)	+ DMSO (1 mM)	+ SOD (100 μg mL^{-1})	λ_{Em}/nm	$^a K_{SV}$/%$^{-1}$
Ru1	33.7	34.8	2.7	588	0.080 ± 0.0012
Ru2	30.5	32.7	2.3	588	0.044 ± 0.0013

^{a}Mean ± standard deviation (n = 3).

DOI: 10.1021/acs.inorgchem.5b00862
Inorg. Chem. 2015, 54, 8281−8287

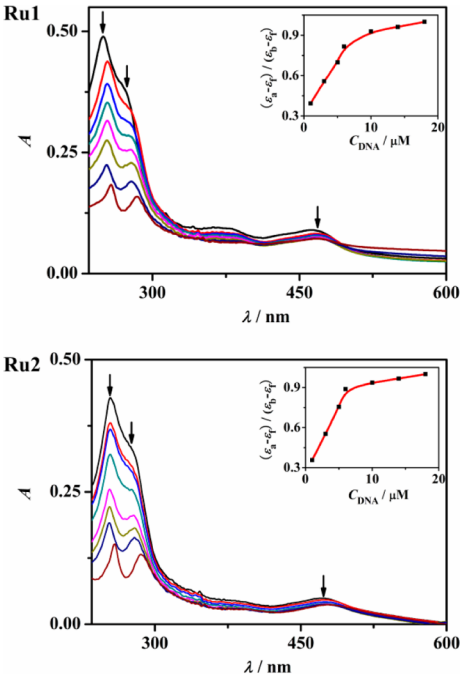

Figure 4. Absorption spectra of 10 μM Ru1 or Ru2 with increasing DNA concentration (C_{DNA}, from 0 to18 μM) under air-containing conditions. Inset shows the relation of $(\varepsilon_a-\varepsilon_f)/(\varepsilon_b-\varepsilon_f)$ with C_{DNA}.

$$b = 1 + K_bC_{Ru} + K_bC_{DNA}/2s \quad (4b)$$

where C_{DNA} is the DNA concentration in nucleotides, and the apparent absorption coefficients ε_a, ε_f, and ε_b correspond to A_{obsd}/C_{Ru}, the absorbance for the free Ru(II) complexes, and the absorbance for the fully bound Ru(II) complexes, respectively. Combined with the nonlinear least-squares analysis (insets of Figure 4), the K_b values are 7.9×10^4 M^{-1} (s = 2.7) and 3.3×10^5 M^{-1} (s = 3.7) for Ru1 and Ru2, respectively (correlation coefficient $R^2 > 0.98$). These K_b values are in the same order of those reported previously for $[Ru(bpy)_2(HNAIP)]^{2+}$ (8.3×10^4 M^{-1}) and $[Ru(bpy)_2(HPIP)]^{2+}$ (6.5×10^5 M^{-1}), respectively,[29] whereas they are far smaller than that of $[Ru(IP)_2(dppz)]^{2+}$ (2.1×10^7 M^{-1} and s = 0.4),[30] and larger than that of $[Ru(bpy)_2(IP)]^{2+}$ (4.1×10^4 M^{-1}),[46] suggesting a moderate DNA binding.

It is worthy of note that the DNA binding constant of Ru1 is smaller than that of Ru2. Meanwhile, the presence of 18 μM DNA leads to a red shift of 2 and 6 nm for the MLCT absorption peak of Ru1 and Ru2, revealed by absorption spectra, and the emission intensities of Ru1 and Ru2 under an air-containing atmosphere are enhanced by 48% and 129%, respectively, as shown by Figure 5. In addition, the time-resolved spectra show that the emission lifetime ratios ($\tau_{Ru\text{-}DNA}/\tau_{Ru}$) of Ru1 and Ru2 in the presence and absence of 8.3 μM DNA under a pure nitrogen atmosphere are 0.79 and 1.22 for Ru1 and Ru2, respectively (Figure 6), implying the self-quenching of Ru1 bound to DNA.[47] The results suggest that Ru2 has stronger affinity to DNA than Ru1 possessing a 2-hydroxynaphthalene π-conjugated plane. Combined with the DNA binding of $[Ru(bpy)_2(HNAIP)]^{2+}$ and $[Ru(bpy)_2(HPIP)]^{2+}$,[29] and the structure of 2-phenylimidazo[4,5-f]-[1,10]phenanthroline (PIP) revealed by single-crystal X-ray diffraction, in which the phenyl ring is almost coplanar with IP,[48] we speculate that the resorcinol of DHPIP may be closely coplanar with IP due to the formation of an intramolecular

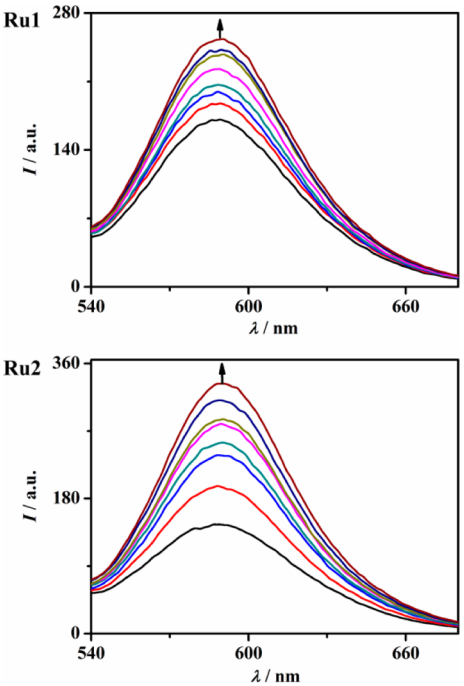

Figure 5. Emission spectra of 10 μM Ru1 or Ru2 under an air-containing atmosphere with increasing C_{DNA} from 0 to 18 μM.

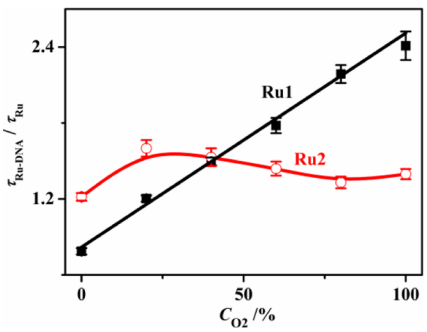

Figure 6. $\tau_{Ru\text{-}DNA}/\tau_{Ru}$ ratios of 10 μM Ru1 or Ru2 in the absence and presence of 8.3 μM DNA as a function of C_{O_2}.

hydrogen bond, and the 2-hydroxynaphthyl ring has potential to lie out of the plane of IP by the rotatable C−C single bond.[49,50] As a result, Ru1 and Ru2 are suggested to bind DNA via groove-binding and intercalation modes, respectively.

3.3. DNA Conformational Transition Induced by Groove Binding of Ru1. To further distinguish the DNA-binding modes between Ru1 and Ru2, the CD spectra of DNA upon increasing the concentration of Ru1 and Ru2 were measured. As depicted by Figure 7, the DNA (0.04 mM) shows two conservative CD bands, i.e., a major positive band from base stacking at 276 nm and a right handed helicity-based negative band at 246 nm (solid line).[51] While adding Ru1 and Ru2 of 0.024 mM (dotted line) or 0.048 mM (dashed line), the former CD spectra show a dramatic change. As the negative band at 246 nm is suppressed, the major positive band is divided into a positive band at 261 nm and a negative band at 287 nm, which are virtually identical with the CD spectra of the Z-DNA described in previous studies.[28] The results suggest that Ru1 may act as a "wedge" to pry the DNA groove, and further allow the double helix to bend the left in a zigzag pattern,[52] resulting in the B-to-Z conformation transition to form the Z-

DOI: 10.1021/acs.inorgchem.5b00862
Inorg. Chem. 2015, 54, 8281−8287

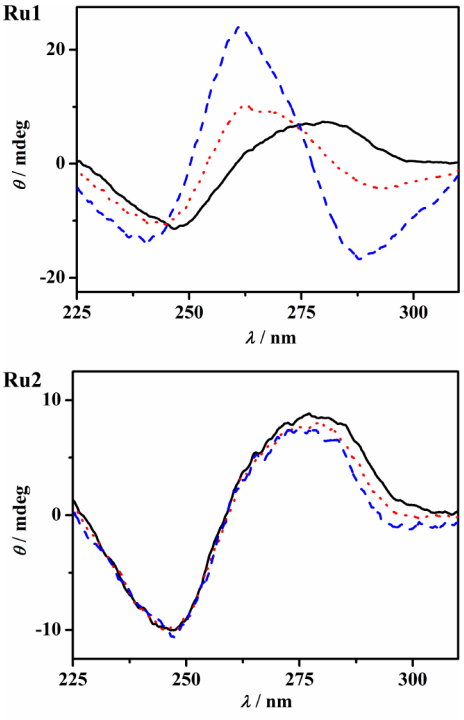

Figure 7. CD spectra of 0.04 mM DNA in the absence (solid line) and presence of Ru1 or Ru2 of 24 μM (dotted line) and 48 μM (dashed line).

DNA stabilized by Ru1. It is worthy of note that there is no pronounced effect of low concentration of Ru2 on the DNA conformation under an analogous condition. Combined with all the results from spectroscopic titrations, it is reasonably inferred that Ru1 and Ru2 can bind DNA via groove-binding and intercalation modes, respectively, and Ru1 has the ability to induce the B-to-Z DNA conformation transition.

3.4. Effects of DNA Conformation on Oxygen-Sensing Performance. In the previous studies, the intercalation of the photoexcited $[Ru(bpy)_2(ddz)]^{2+}$ (ddz = dibenzo[*h*,*j*]dipyrido-[3,2-*a*:2′,3′-*c*]phenazine) to the high concentration of DNA ($r = C_{DNA}/C_{Ru} = 50$) has been found to increase the emission lifetimes under an oxygen atmosphere.[53] Although a high DNA-to-Ru molar ratio facilitates the full binding of Ru(II) complexes to DNA, an excess of DNA may disturb the binding of photoexcited Ru(II) complexes to oxygen. In this study, the DNA concentration was fixed at 8.3 μM for 10 μM Ru(II) complexes due to the formation of a $[Ru(bpy)_2(dppz)]^{2+}$-intercalated cast film stably existing in buffer solutions at r = 0.83.[54] As shown in Figure 6, we have comparatively investigated the effects of increasing concentration of oxygen on the $\tau_{Ru\text{-}DNA}/\tau_{Ru}$ ratios of Ru1 and Ru2 in the absence and presence of 8.3 μM DNA (r = 0.83). The $\tau_{Ru\text{-}DNA}/\tau_{Ru}$ values of Ru1 show a linear increase with increasing oxygen concentration, whereas those for Ru2 only show a slight change, suggesting that DNA protects the photoexcited Ru1 from oxygen quenching.

To further illustrate the oxygen quenching performance of Ru1 and Ru2 in the presence of 8.3 μM DNA, the steady-state and time-resolved emission spectra were measured. As depicted by Figures 8 and 9, a very interesting phenomenon is observed. The emission intensities of Ru1 and Ru2 bound to DNA show a linear decrease with increasing oxygen concentration. The K_{SV} values of Ru1 and Ru2 bound to DNA are 0.017 $\%^{-1}$ and 0.045

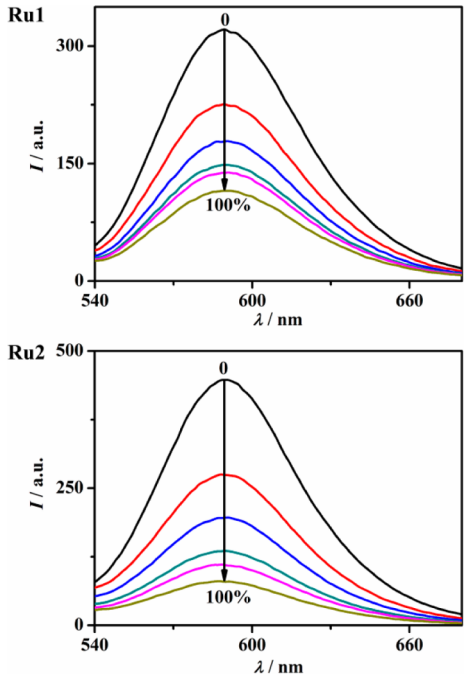

Figure 8. Emission spectra of 10 μM Ru1 or Ru2 in the presence of 8.3 μM DNA with increasing C_{O_2} (from curves 1−6): 0, 20, 40, 60, 80, and 100%.

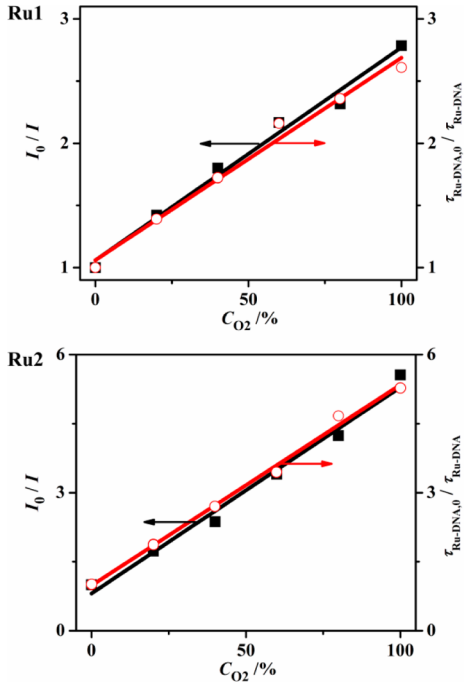

Figure 9. I_0/I (left) and $\tau_{Ru\text{-}DNA,0}/\tau_{Ru\text{-}DNA}$ (right) of 10 μM Ru1 or Ru2 in the presence of 8.3 μM DNA under pure nitrogen and increasing C_{O_2} atmospheres as a function of C_{O_2}.

$\%^{-1}$, and their I_0/I_{100} ratios are 2.8 and 5.6, respectively. The presence of DNA largely decreases the K_{SV} and I_0/I_{100} ratio of Ru1, whereas there is no pronounced effect on those of Ru2. The $\tau_{Ru\text{-}DNA,0}/\tau_{Ru\text{-}DNA}$ ratios show a linear increase with increasing oxygen concentration (Figure 9), suggesting a dynamic emission quenching, which is consistent with the case in the absence of DNA. However, the k_q value of Ru1

DOI: 10.1021/acs.inorgchem.5b00862
Inorg. Chem. 2015, 54, 8281−8287

bound to the groove surface of DNA is decreased by 33% in contrast to that without DNA, and the k_q value of Ru2 is hardly weakened by DNA. The results suggest that the presence of the Z-DNA conformation may weaken the oxygen-responsive emission of Ru1. It can be concluded for the reasons as described below.

In the presence of 8.3 μM DNA, there exists a binding equilibrium of Ru1 and Ru2 with DNA via groove-binding and intercalation modes, respectively. The curve 1 in Figure 8 shows the average photoluminescence from bound and free Ru(II) complexes. While injecting oxygen into the test solutions, a new binding equilibrium appears between oxygen and photoexcited Ru(II) complexes free or bound to DNA, leading to the dynamic emission quenching (curves 2–6 of Figure 8, and Figure 9). On the time scale of photoluminescence measurement, the emission quenching of Ru1 and Ru2 by oxygen in the absence and presence of DNA conforms to the Stern–Volmer equation.[55] However, as depicted by Figure 1, Ru1 can bind to the groove surface of DNA to induce the B-to-Z conformation transition, resulting in the Z-DNA stabilized by Ru1. Because the Z-DNA is quite different from the B-DNA, in which B-DNA has major and minor grooves with widths of 1.17 and 0.57 nm, and Z-DNA only shows basically consistent minor grooves with B-DNA,[56] the oxygen binding rates across the two kinds of conformational DNA would be different. The oxygen molecules in buffer solutions can pass through B-DNA without hindrance to bind the photoexcited Ru2, making the oxygen quenching rate hardly change. The Z-DNA may block the interaction of the photoexcited Ru1 with oxygen due to the zigzag structure without major grooves, leading to a decrease of about 33% for Ru1-based oxygen-sensing rate.

4. CONCLUSIONS

In summary, Ru1 shows a good linear response toward oxygen between pure nitrogen and pure oxygen with an I_0/I_{100} ratio of up to 9.3 via a dynamic quenching mechanism. Compared with Ru2 (I_0/I_{100} = 5.8), the HNAIP ligand endows Ru1 with favorable oxygen binding sites to achieve larger energy and electron transfer rates. On the other hand, Ru1 can bind to the groove surface of DNA ($K_b = 7.9 \times 10^4$ M^{-1}) to induce the B-to-Z conformational transition, which is not observed for Ru2 intercalated into DNA ($K_b = 3.3 \times 10^5$ M^{-1}). In addition, the B-to-Z DNA conformational transition is interestingly found to decrease the Ru1-based oxygen-sensing rate by about 33%. The present results should be of value for better understanding the interactions between DNA and polypyridyl Ru(II) complexes, as well as offer a new approach to evaluate the oxygen-sensing properties of DNA binders.

AUTHOR INFORMATION

Corresponding Author

*Fax: +86 20 39310187. E-mail: lihong@scnu.edu.cn.

Notes

The authors declare no competing financial interest.

ACKNOWLEDGMENTS

This work was supported by the National Natural Science Foundation of China (No. 21271075) and the Natural Science Foundation of Guangdong Province (No. 10351063101000001).

REFERENCES

(1) Jaenisch, R.; Bird, A. *Nat. Genet.* **2003**, *33*, 245–254.
(2) Rich, A.; Nordheim, A.; Wang, A. H. *Annu. Rev. Biochem.* **1984**, *53*, 791–846.
(3) Hamada, H.; Kakunaga, T. *Nature* **1982**, *298*, 396–398.
(4) Wang, G.; Vasquez, K. M. *Front. Biosci.* **2007**, *12*, 4424–4438.
(5) Li, H.; Xiao, J.; Li, J. M.; Lu, L.; Feng, S.; Droge, P. *Nucleic Acids Res.* **2009**, *37*, 2737–2746.
(6) Kim, Y. G.; Park, H. J.; Kim, K. K.; Lowenhaupt, K.; Rich, A. *Nucleic Acids Res.* **2006**, *34*, 4937–4942.
(7) Yang, L.; Wang, S.; Tian, T.; Zhou, X. *Curr. Med. Chem.* **2012**, *19*, 557–568.
(8) Zhang, A. G.; Zhang, Y. Z.; Duan, Z. M.; Wang, K. Z.; Wei, H. B.; Bian, Z. Q.; Huang, C. H. *Inorg. Chem.* **2011**, *50*, 6425–6436.
(9) Sun, B.; Guan, J. X.; Xu, L.; Yu, B. L.; Jiang, L.; Kou, J. F.; Wang, L.; Ding, X. D.; Chao, H.; Ji, L. N. *Inorg. Chem.* **2009**, *48*, 4637–4639.
(10) Hall, J. P.; Cook, D.; Morte, S. R.; McIntyre, P.; Buchner, K.; Beer, H.; Cardin, D. J.; Brazier, J. A.; Winter, G.; Kelly, J. M.; Cardin, C. J. *J. Am. Chem. Soc.* **2013**, *135*, 12652–12659.
(11) Wu, Z. G.; Tian, T.; Yu, J. P.; Weng, X. C.; Liu, Y.; Zhou, X. *Angew. Chem., Int. Ed.* **2011**, *50*, 11962–11967.
(12) Maheswari, P. U.; Rajendiran, V.; Palaniandavar, M.; Parthasarathi, R.; Subramanian, V. A. *Bull. Chem. Soc. Jpn.* **2005**, *78*, 835–844.
(13) Valko, M.; Leibfritz, D.; Moncol, J.; Cronin, M. T. D.; Mazur, M.; Telser, J. *Int. J. Biochem. Cell Biol.* **2007**, *39*, 44–84.
(14) Jorge, P. A. S.; Caldas, P.; Rosa, C. C.; Oliva, A. G.; Santos, J. L. *Sens. Actuators, B* **2004**, *103*, 290–299.
(15) Ji, J.; Rosenzweig, N.; Jones, I.; Rosenzweig, Z. *J. Biomed. Opt.* **2002**, *7*, 404–409.
(16) Fiore, G. L.; Goguen, B. N.; Klinkenberg, J. L.; Payne, S. J.; Demas, J. N.; Fraser, C. L. *Inorg. Chem.* **2008**, *47*, 6532–6540.
(17) Zhang, H. R.; Li, B.; Lei, B. F.; Li, W. L.; Lu, S. Z. *Sens. Actuators, B* **2007**, *123*, 508–515.
(18) Lei, B. F.; Li, B.; Zhang, H. R.; Zhang, L. M.; Li, W. L. *J. Phys. Chem. C* **2007**, *111*, 11291–11301.
(19) Zheng, H. Z.; Zu, Y. B. *J. Phys. Chem. B* **2005**, *109*, 12049–12053.
(20) Abdel-Shafi, A. A.; Ward, M. D.; Schmidt, R. *Dalton T.* **2007**, 2517–2527.
(21) Grusenmeyer, T. A.; Chen, J.; Jin, Y.; Nguyen, J.; Rack, J. J.; Schmehl, R. H. *J. Am. Chem. Soc.* **2012**, *134*, 7497–7506.
(22) Bukowski, R. M.; Ciriminna, R.; Pagliaro, M.; Bright, F. V. *Anal. Chem.* **2005**, *77*, 2670–2672.
(23) Carraway, E. R.; Demas, J. N.; DeGraff, B. A.; Bacon, J. R. *Anal. Chem.* **1991**, *63*, 337–342.
(24) Ji, S. M.; Wu, W. H.; Wu, W. T.; Song, P.; Han, K. L.; Wang, Z. G.; Liu, S. S.; Guo, H. M.; Zhao, J. Z. *J. Mater. Chem.* **2010**, *20*, 1953–1963.
(25) Wu, W. H.; Ji, S. M.; Wu, W. T.; Guo, H. M.; Wang, X.; Zhao, J. Z.; Wang, Z. G. *Sens. Actuators, B* **2010**, *149*, 395–406.
(26) Amao, Y.; Okura, I. *Sens. Actuators, B* **2003**, *88*, 162–167.
(27) Friedman, A. E.; Kumar, C. V.; Turro, N. J.; Barton, J. K. *Nucleic Acids Res.* **1991**, *19*, 2595–2602.
(28) Gan, G. L.; Chao, H.; Cai, X. P.; Jiang, Z. S.; Li, H. *J. Inorg. Biochem.* **2013**, *129*, 9–14.
(29) Liu, J. G.; Ye, B. H.; Li, H.; Zhen, Q. X.; Ji, L. N.; Fu, Y. H. *J. Inorg. Biochem.* **1999**, *76*, 265–271.
(30) Liu, J. G.; Ye, B. H.; Li, H.; Ji, L. N.; Li, R. H.; Zhou, J. Y. *J. Inorg. Biochem.* **1999**, *73*, 117–122.
(31) Wu, J. Z.; Ye, B. H.; Wang, L.; Ji, L. N.; Zhou, J. Y.; Li, R. H.; Zhou, Z. Y. *J. Chem. Soc., Dalton Trans.* **1997**, 1395–1402.
(32) Sharman, K. K.; Periasamy, A.; Ashworth, H.; Demas, J. N; Snow, N. H. *Anal. Chem.* **1999**, *71*, 947–952.
(33) Zheng, L. Y.; Chi, Y. W.; Shu, Q. Q.; Dong, Y. Q.; Zhang, L.; Chen, G. N. *J. Phys. Chem. C* **2009**, *113*, 20316–20321.
(34) Oter, O.; Ertekin, K.; Derinkuyu, S. *Mater. Chem. Phys.* **2009**, *113*, 322–328.

DOI: 10.1021/acs.inorgchem.5b00862
Inorg. Chem. 2015, 54, 8281–8287

(35) Wang, Y. Y.; Li, B.; Zhang, L. M.; Song, H. *Langmuir* **2013**, *29*, 1273−1279.
(36) Ruggi, A.; van Leeuwen, F. W. B.; Velders, A. H. *Coord. Chem. Rev.* **2011**, *255*, 2542−2554.
(37) Choi, M. M. F.; Xiao, D. *Anal. Chim. Acta* **1999**, *387*, 197−205.
(38) Wang, B.; Liu, Y.; Li, B.; Yue, S.; Li, W. *J. Lumin.* **2008**, *128*, 341−347.
(39) Morris, K. J.; Roach, M. S.; Xu, W. Y.; Demas, J. N.; DeGraff, B. A. *Anal. Chem.* **2007**, *79*, 9310−9314.
(40) Rehman, A. U.; Cser, K.; Sass, L.; Vass, I. *Biochim. Biophys. Acta, Bioenerg.* **2013**, *1827*, 689−698.
(41) Liu, N.; Sun, G. *Ind. Eng. Chem. Res.* **2011**, *50*, 5326−5333.
(42) Cruz, A. J.; Kirgan, R.; Siam, K.; Heiland, P.; Rillema, D. P. *Inorg. Chim. Acta* **2010**, *363*, 2496−2505.
(43) Pierlot, C.; Hajjam, S.; Barthélémy, C.; Aubry, J. M. *J. Photochem. Photobiol., B* **1996**, *36*, 31−39.
(44) Ambrosek, D.; Loos, P. F.; Assfeld, X.; Daniel, C. *J. Inorg. Biochem.* **2010**, *104*, 893−901.
(45) Gan, G. L.; Chao, H.; Ji, S. B.; Chen, L. L.; Li, H. *Spectrochim. Acta, Part A* **2012**, *97*, 297−305.
(46) Wu, J.-Z.; Li, L.; Zeng, T.-X.; Ji, L.-N.; Zhou, J.-Y.; Luo, T.; Li, R.-H. *Polyhedron* **1997**, *16*, 103−107.
(47) Poulin, K. W.; Smirnov, A. V.; Hawkins, M. E.; Balis, F. M.; Knutson, J. R. *Biochemistry* **2009**, *48*, 8861−8868.
(48) Wang, X. L.; Chen, Y. Q.; Liu, G. C.; Lin, H. Y.; Zhang, J. X. *J. Solid State Chem.* **2009**, *182*, 2392−2401.
(49) Liu, J. G.; Ye, B. H.; Zhang, Q. L.; Zou, X. H.; Zhen, Q. X.; Tian, X.; Ji, L. N. *JBIC, J. Biol. Inorg. Chem.* **2000**, *5*, 119−128.
(50) Płotek, M.; Starosta, R.; Nitek, W.; Komarnicka, U. K.; Stochel, G.; Kyzioł, A. *Polyhedron* **2014**, *68*, 357−364.
(51) Sathyaraj, G.; Weyhermuller, T.; Nair, B. U. *Eur. J. Med. Chem.* **2010**, *45*, 284−291.
(52) McDonnell, U.; Hicks, M. R.; Hannon, M. J.; Rodger, A. *J. Inorg. Biochem.* **2008**, *102*, 2052−2059.
(53) Hergueta-Bravo, A.; Jiménez-Hernández, M. E.; Montero, F.; Oliveros, E.; Orellana, G. *J. Phys. Chem. B* **2002**, *106*, 4010−4017.
(54) Chen, M. J.; Li, H.; Shao, J. Y.; Huang, Y.; Xu, Z. H. *Inorg. Chem.* **2011**, *50*, 2043−2045.
(55) Taheri, A.; Meyer, G. J. *Dalton T.* **2014**, *43*, 17856−17863.
(56) Wang, A. H.; Quigley, G. J.; Kolpak, F. J.; Crawford, J. L.; van Boom, J. H.; van der Marel, G.; Rich, A. *Nature* **1979**, *282*, 680−686.

DOI: 10.1021/acs.inorgchem.5b00862
Inorg. Chem. 2015, 54, 8281−8287